Available online at www.sciencedirect.com

ScienceDirect

Nuclear Physics B 899 (2015) 547–569

NUCLEAR PHYSICS B

www.elsevier.com/locate/nuclphysb

Studying the perturbed Wess–Zumino–Novikov–Witten $SU(2)_k$ theory using the truncated conformal spectrum approach

R.M. Konik [a], T. Pálmai [b], G. Takács [b,c,*], A.M. Tsvelik [a]

[a] *Department of Condensed Matter Physics and Materials Science, Brookhaven National Laboratory, Upton, NY 11973-5000, USA*

[b] *MTA-BME "Momentum" Statistical Field Theory Research Group, H-1111 Budapest, Budafoki út 8, Hungary*

[c] *Department of Theoretical Physics, Institute of Physics, Budapest University of Technology and Economics, H-1111 Budapest, Budafoki út 8, Hungary*

Received 19 May 2015; received in revised form 14 August 2015; accepted 19 August 2015

Available online 24 August 2015

Editor: Hubert Saleur

Abstract

We study the $SU(2)_k$ Wess–Zumino–Novikov–Witten (WZNW) theory perturbed by the trace of the primary field in the adjoint representation, a theory governing the low-energy behavior of a class of strongly correlated electronic systems. While the model is non-integrable, its dynamics can be investigated using the numerical technique of the truncated conformal spectrum approach combined with numerical and analytical renormalization groups (TCSA + RG). The numerical results so obtained provide support for a semiclassical analysis valid at $k \gg 1$. Namely, we find that the low energy behavior is sensitive to the sign of the coupling constant, λ. Moreover, for $\lambda > 0$ this behavior depends on whether k is even or odd. With k even, we find definitive evidence that the model at low energies is equivalent to the massive O(3) sigma model. For k odd, the numerical evidence is more equivocal, but we find indications that the low energy effective theory is critical.

* Corresponding author.
E-mail address: takacsg@eik.bme.hu (G. Takács).

http://dx.doi.org/10.1016/j.nuclphysb.2015.08.016

1. Introduction

Conformal field theories (CFT) describe universal critical behavior and by virtue of this play an enormously important role in the physics of strongly correlated systems. This universality is not completely lost in the presence of perturbations since, as a rule, the number of relevant operators is finite and once restricted by symmetry, often number but a few. Physics of perturbed critical models can be rich and complex, especially when the perturbation is non-integrable. For examples one may look at the quantum Ising model perturbed simultaneously by a longitudinal magnetic field and the thermal operator [1,2] or double sine-Gordon models [3,4].

A focus on relevant perturbations of a CFT is most appropriate when the perturbations are strongly relevant. Indeed, the more relevant the perturbation the smaller is the energy scale over which the spectrum is significantly altered. This feature lies at the foundation of the truncated conformal spectrum approach (TCSA) introduced in [5]. In the simplest version of this approach (TCSA), one truncates the spectrum of the unperturbed CFT which reduces the problem to numerical diagonalization of finite size matrices. Later this idea was combined with a numerical renormalization group [6] (TCSA + NRG). The TCSA + NRG has been used to tackle a number of problems ranging from the excitonic spectrum in semiconducting carbon nanotubes [7,8], to quenches in the Lieb–Liniger model [9,10], to studying theories whose fields live on a non-compact manifold [11]. In a further development, the precision of TCSA or TCSA + NRG computations can be improved further upon using perturbative renormalization group techniques [7,8,12–15]. These same renormalization group techniques allow one to use the TCSA to predict gaps in actual material systems which possess a finite bandwidth/cutoff [8].

Below we will apply the TCSA + NRG to study the $(1+1)$-dimensional $SU(2)_k$ Wess–Zumino–Novikov–Witten (WZNW) model perturbed by the trace of the adjoint operator. This is a strongly relevant operator with scaling dimension $d = \frac{4}{k+2}$ ideal for application of the TCSA + NRG method. This perturbed conformal field theory appears in applications such as theories of spin ladders [16] (see also Appendix A). A variant of this theory, perturbing $SU(2)_k$ by the trace of the adjoint on the boundary of the system, describes a particular class of Kondo models [17]. Another variant of the model, with an additional current–current perturbation, appeared in the description of fermionic cold atoms loaded into a one-dimensional optical lattice [18,19].

The perturbed CFT is not integrable except at $k = 2$ when it is equivalent to the theory of three massive Majorana fermions. Below we will use the semiclassical approximation to analyze the case of $k \gg 1$ while using TCSA + NRG for small finite values of k. Our investigations yield concrete predictions for the vacuum structure and low-energy excitations for systems described by this perturbed conformal field theory.

The most striking property of the theory is the dependence of its properties on the sign of the coupling constant, λ. For $\lambda > 0$ there is a dichotomy in behavior between even and odd k. For odd k the semiclassical analysis predicts a massless RG flow from the $SU(2)_k$ critical point to $SU(2)_1$ in the infrared. The spectrum for even k is always massive and the lowest multiplet is a triplet. However the size of the mass depends on the sign of λ so that the mass is smaller for $\lambda > 0$ with the ratio $m(-\lambda)/m(\lambda)$ increasing exponentially with k.

2. The perturbed $SU(2)_k$ WZNW model

The model in which we are interested is the $SU(2)_k$ WZNW model perturbed by the trace of the primary field in the adjoint representation:

$$S = kW(g) + \lambda \sum_{a=1}^{3} \int d^2x \, \mathrm{Tr}[\sigma^a g \sigma^a g^+]; \tag{1}$$

$$W(g) = \frac{1}{16\pi} \int d^2x \, \mathrm{Tr}(\partial^\mu g^\dagger \partial_\mu g) + \Gamma(g);$$

$$\Gamma(g) = \frac{1}{24\pi} \int_B d^3y \, \epsilon^{\alpha\beta\gamma} \, \mathrm{Tr}(g^\dagger \partial_\alpha g g^\dagger \partial_\beta g g^\dagger \partial_\gamma g), \tag{2}$$

where $\Gamma(g)$ is the famous Wess–Zumino term and σ^a are the Pauli matrices. The perturbation is equivalent to the trace of the WZNW principal field in the adjoint representation:

$$\mathrm{Tr}[\sigma^a g \sigma^b g^\dagger] \sim \Phi^{ab}_{adj}. \tag{3}$$

This is a strongly relevant operator with scaling dimension $d = \frac{4}{k+2}$ and as such it generates a characteristic energy scale

$$m \sim |\lambda|^{1/(2-d)}, \tag{4}$$

below which the spectrum is strongly modified.

It is interesting to note that the model perturbed by a single component of matrix Φ_{adj} is integrable. It was demonstrated in [21] that the perturbed Hamiltonian decomposes into a massless U(1) CFT and a massive Z_k CFT perturbed by the thermal operator. The properties of the latter massive theory were studied in [21,22]. However with the inclusion of the entire trace, integrability is lost for $k > 2$. At $k = 2$ the model is equivalent to the model of three massive Majorana fermions with mass $m \sim \lambda$. In this form it has been used to describe the spin $S = 1$ spin ladder [20].

It is interesting to note that for $k = 4$ when the central charge of the critical WZNW theory is equal to $c = 2$, the model can be recast in abelian form:

$$S = \int d^2x \Big[\frac{1}{8\pi} \sum_{a=1,2} (\partial_\mu \phi_a)^2 - \lambda \sum_{i=1}^{3} \cos\left(e_a^{(i)} \phi_a\right) \Big],$$

$$\left(\mathbf{e}^{(i)}\right)^2 = 2/3, \quad \left(\mathbf{e}^{(i)} \mathbf{e}^{(j)}\right) = -1/3, \tag{5}$$

as well as the $SU(3)_1$ WZNW model perturbed by the trace of the matrix operator:

$$S = W[SU(3); g] + \lambda \, \mathrm{Tr}(g + g^\dagger). \tag{6}$$

To get a qualitative understanding of the spectrum of model (Eqn. (1)), we consider the case $k \gg 1$ where the model can be treated semiclassically. Using the identity

$$\sum_{a=1}^{3} \mathrm{Tr}[\sigma^a g \sigma^a g^\dagger] = 2 \, \mathrm{Tr} \, g \, \mathrm{Tr} \, g^\dagger - 2 \tag{7}$$

and the fact that the $SU(2)$ matrix g can be written as

$$g = n_0 \hat{I} + \mathrm{i} \sigma^a n^a, \quad n_0^2 + \mathbf{n}^2 = 1, \tag{8}$$

we obtain the perturbation in the form

$$\sum_a \mathrm{Tr}[\sigma^a g \sigma^a g^\dagger] = \sum_a \Phi^{aa}_{adj} = 2n_0^2. \tag{9}$$

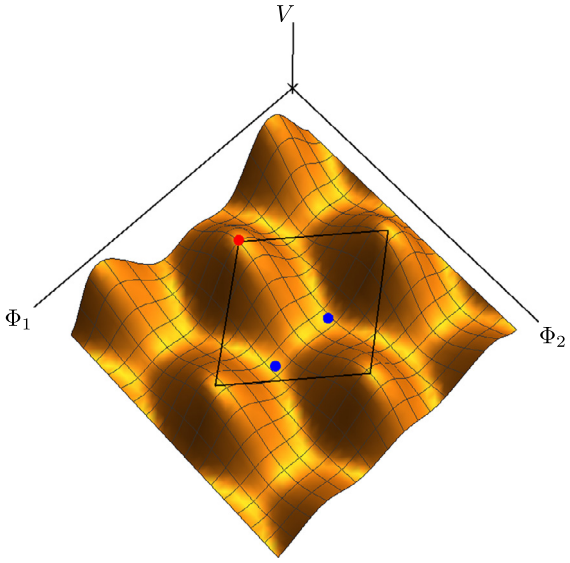

Fig. 1. The potential surface for $k = 4$. The black lines show the elementary cell of the periodic potential, blue dots show the two minima relevant for $\lambda < 0$ that are connected via a saddle point. The red dot is a maximum of the potential, which becomes the only minimum (per elementary cell) for $\lambda > 0$. (For interpretation of the references to color in this figure, the reader is referred to the web version of this article.)

For $\lambda < 0$ the ground state is doubly degenerate, i.e. $n_0 = \pm 1$. (For the $SU(3)$ model (Eqn. (6)) this degeneracy corresponds to two possible choices of the g matrix: $g = e^{\pm 2\pi i/3} I$.) For a given choice of the sign one can consider deviations of the field g from the vacuum configuration as small. Then the low energy theory becomes a theory of three weakly interacting bosons with a Lagrangian density given by

$$\mathcal{L}_{\mathit{eff}} = \frac{k}{4\pi}(\partial_\mu \mathbf{n})^2 + 2|\lambda|\mathbf{n}^2 + \ldots \tag{10}$$

where the dots stand for higher order terms. By rescaling $n^a \to n^a/k^{1/2}$ we see that these terms contain powers of $k^{-1} \ll 1$. Here the mass scale,

$$m \sim \sqrt{\frac{|\lambda|}{k}}, \tag{11}$$

is obviously the one which is envisaged by RG considerations as $k \to \infty$ (see Eqn. (4)). The double degeneracy of the vacuum is in agreement with the structure of the potential in the abelian action (Eqn. (5)), which is periodic under translations with a two-dimensional lattice generated by the vectors $\mathbf{e}^{(i)}$ with two minima in each elementary cell, as shown in Fig. 1.

For $\lambda > 0$ the situation becomes more interesting. At energies below m, the field n_0 is suppressed and $\mathbf{n}$ becomes a unit vector. As a consequence the Wess–Zumino term (2) becomes a topological one [28,29]:

$$\Gamma(\mathrm{i}\sigma^a n^a) = \frac{\mathrm{i}}{8}\int d^2x \epsilon_{\mu\nu}\Big(\mathbf{n}[\partial_\mu \mathbf{n} \times \partial_\nu \mathbf{n}]\Big) \equiv \mathrm{i}\pi\Theta. \tag{12}$$

The coefficient of the topological term in (1) is πk. Since the value of Θ is always integer, $ik\pi\Theta$ contributes nontrivially to the action only when k is odd. In summary, the low energy effective action for $\lambda > 0$ is

$$S = \frac{k}{4\pi}\int d^2x(\partial_\mu \mathbf{n})^2 + i\pi k\Theta, \quad \mathbf{n}^2 = 1. \tag{13}$$

This model is exactly solvable. For k even [30,31] the particles are massive triplets with mass

$$M_{tr} \sim mk\exp(-k/2), \quad m \sim \lambda^{1/2}. \tag{14}$$

The triplet structure of the particle multiplet agrees with the result for $k = 2$. However note that the mass scale at $\lambda > 0$ is much smaller than the RG scale (Eqn. (4)). For k odd, the scale m (14) marks instead a crossover into a basin of attraction of the critical point of the $SU(2)_1$ WZNW model [32].

3. TCSA for the perturbed WZNW model

3.1. The truncated conformal space approach for $SU(2)_k$ perturbed by the trace of adjoint

For a numerical determination of the spectrum we use the truncated conformal space approach [5], adapted to the $SU(2)_k$ WZNW model. For perturbations of WZNW models with levels $k = 1$ and 2 TCSA was applied previously in [33]; for the present work we developed a general purpose TCSA code working for all k and any perturbing operator. On a Euclidean space–time cylinder of circumference, R, in the spatial direction, x, the Hamiltonian has the form,

$$H = H_k + \lambda\int_0^R dx\,\Phi(0,x), \tag{15}$$

where H_k is the Hamiltonian of the $SU(2)_k$ WZNW model (Eqn. (2)) and the perturbing operator Φ is minus the trace of the adjoint field (Eqn. (3)). Due to translation invariance, the Hamiltonian is block-diagonal on eigenspaces of the conformal spin $L_0 - \bar{L}_0$. The symmetry algebra is generated by Kac–Moody currents, $J^\alpha(z)$, which satisfy the OPE,

$$J^\alpha(z)J^\beta(w) = \frac{k}{2}\frac{q^{\alpha\beta}}{(z-w)^2} + \frac{f_\gamma^{\alpha\beta}J^\gamma(w)}{z-w} + O(1), \tag{16}$$

where $q^{\alpha\beta}$ is the invariant metric of the Lie-algebra $su(2)$, and $f_\gamma^{\alpha\beta}$ are the structure constants. In the basis, $\{S^0, S^\pm\}$, the $su(2)$ algebra relations can be written as

$$\begin{aligned}&[S^\alpha, S^\beta] = f_\gamma^{\alpha\beta}S^\gamma, \qquad f_\gamma^{\alpha\beta} = 0 \qquad \alpha+\beta\neq\gamma;\\ &\qquad f_+^{0+} = -f_+^{+0} = -f_-^{0-} = f_-^{-0} = 1; \qquad f_0^{+-} = -f_0^{-+} = 2,\end{aligned} \tag{17}$$

and the metric is

$$\begin{aligned}&q^{\alpha\beta} = 0 \qquad \alpha+\beta\neq 0;\\ &q^{00} = 1; \qquad q^{\pm\mp} = 2.\end{aligned} \tag{18}$$

The modes of the current obey the Kac–Moody algebra,

$$J_n^\alpha(z) = \oint_z \frac{d\zeta}{2\pi i}(\zeta - z)^n J^\alpha(\zeta);$$

$$[J_n^\alpha, J_m^\beta] = f_\gamma^{\alpha\beta} J_{n+m}^\gamma + \frac{k}{2} m q^{\alpha\beta}\delta_{n+m,0} \tag{19}$$

(where z denotes an arbitrary reference point of insertion; whenever omitted, it is taken to be $z = 0$). The energy–momentum tensor is given by the Sugawara construction,

$$T(z) = \frac{1}{k+2} q_{\alpha\beta} {:}J^\alpha(z) J^\beta(z){:};$$

$$L_n(z) = \oint_z \frac{d\zeta}{2\pi i}(\zeta - z)^{n+1} T(\zeta) = \frac{q_{\alpha\beta}}{k+2} \sum_{m\in\mathbb{Z}} {:}J_m^\alpha J_{n-m}^\beta{:}, \tag{20}$$

where the modes L_n satisfy the Virasoro algebra,

$$[L_n, L_m] = L_{n+m} + \frac{c}{12} n(n^2-1)\delta_{n,-m}, \qquad c = \frac{3k}{k+2}. \tag{21}$$

We recall that for level k integer there are $k-1$ primary field multiplets $\Phi_{m,\bar m}^{(j)}(z,\bar z)$, with $j = 0, 1/2, \ldots, k/2$ and $m, \bar m = -j, -j+1, \ldots, j$. They are normalized as

$$\langle \Phi_{m_1,\bar m_1}^{(j_1)\dagger}(z_1,\bar z_1) \Phi_{m_2,\bar m_2}^{(j_2)}(z_2,\bar z_2)\rangle = \delta_{j_1 j_2}\delta_{m_1 m_2}\delta_{\bar m_1 \bar m_2}(z_{12}\bar z_{12})^{-2h(j_1)};$$

$$h(j) = \frac{j(j+1)}{k+2};$$

$$\Phi_{m,\bar m}^{(j)\dagger}(z,\bar z) = (-1)^{2j-m-\bar m}\Phi_{-m,-\bar m}^{(j)}(z,\bar z). \tag{22}$$

The Hilbert space of the conformal field theory is given by

$$\mathcal{H}_k = \bigoplus_j \mathcal{V}_j \otimes \bar{\mathcal{V}}_j, \tag{23}$$

where $\mathcal{V}_j$ is the irreducible representation of $su(2)_k$ with highest weight j, and the bar denotes the antiholomorphic component. The ground state level of the module $\mathcal{V}_j \otimes \bar{\mathcal{V}}_j$ is spanned by the multiplet,

$$|m,\bar m\rangle_j = \Phi_{m,\bar m}^{(j)}(0,0)|0\rangle, \tag{24}$$

where $|0\rangle$ is the $SL(2,\mathbb{C})$ invariant conformal vacuum state. The module is generated by the raising operators J_m^α, $m < 0$; care must be taken to factor out null vectors to obtain the irreducible representation.

We remark that for computational simplicity the left and right Kac–Moody algebras were implemented in the same way. This is in contrast with the usual WZNW formalism, where the fundamental field transforms as

$$g \to g_L g g_R^{-1}. \tag{25}$$

However we take our fields to transform as

$$\Phi_{m,\bar m}^{(j)} \to D^{(j)}(g_L)_{mm'} D^{(j)}(g_R)_{\bar m \bar m'} \Phi_{m',\bar m'}^{(j)}, \tag{26}$$

where $D^{(j)}$ is the $SU(2)$ representation corresponding to spin j. This is related to the usual definition by a contragredient transformation applied to g_R which is equivalent to a redefinition of the basis for $SU(2)$.

The operator product coefficients of primary fields were derived in [34]. Introducing the generating function fields

$$\Phi^{(j)}(x,\bar{x};z,\bar{z}) = \sum_{m,\bar{m}} \sqrt{\binom{2j}{m+j}\binom{2j}{\bar{m}+j}}\, x^{j-m}\bar{x}^{j-\bar{m}}\Phi^{(j)}_{m,\bar{m}}(z,\bar{z}), \tag{27}$$

which have the two-point function,

$$\left\langle \Phi^{(j_1)}(x_1,\bar{x}_1;z_1,\bar{z}_1)\Phi^{(j_2)}(x_2,\bar{x}_2;z_2,\bar{z}_2)\right\rangle = \delta^{j_2}_{j_1}(x_{12}\bar{x}_{12})^{2j_1}(z_{12}\bar{z}_{12})^{-2h(j_1)}, \tag{28}$$

the operator algebra is fully specified by the three-point functions of the primary fields given by

$$\begin{aligned}&\left\langle \Phi^{(j_1)}(x_1,\bar{x}_1,z_1,\bar{z}_1)\Phi^{(j_2)}(x_2,\bar{x}_2,z_2,\bar{z}_2)\Phi^{(j_3)}(x_3,\bar{x}_3,z_3,\bar{z}_3)\right\rangle \\ &\quad = C(j_1,\ j_2,\ j_3)(x_{12}\bar{x}_{12})^{j_1+j_2-j_3}(x_{13}\bar{x}_{13})^{j_1+j_3-j_2}(x_{23}\bar{x}_{23})^{j_2+j_3-j_1} \\ &\qquad \times (z_{12}\bar{z}_{12})^{h(j_3)-h(j_1)-h(j_2)}(z_{13}\bar{z}_{13})^{h(j_2)-h(j_1)-h(j_3)}(z_{23}\bar{z}_{23})^{h(j_1)-h(j_2)-h(j_3)},\end{aligned} \tag{29}$$

where the structure constants C are given by

$$\begin{aligned}&C(j_1,\ j_2,\ j_3)^2 = \gamma\left(\frac{1}{k+2}\right)P(j_1+j_2+j_3+1)^2\prod_{n=1}^{3}\frac{P(j_1+j_2+j_3-2j_n)^2}{\gamma\left(\frac{2j_n+1}{k+2}\right)P(2j_n)^2}; \\ &\gamma(x) = \frac{\Gamma(x)}{\Gamma(1-x)} \qquad P(j) = \prod_{n=1}^{j}\gamma\left(\frac{n}{k+2}\right),\end{aligned} \tag{30}$$

and are fully symmetric in their arguments. Structure constants for component fields can be obtained by expanding in the variables $x,\bar{x}$ and using Eqn. (27).

The trace of the adjoint field can be expressed as the component of the $j=1$ field which is a singlet under the global $SU(2)$ symmetry generated by $J^a_0+\bar{J}^a_0$:

$$\Phi = \frac{1}{\sqrt{3}}\left(\Phi^{(1)}_{1,-1}+\Phi^{(1)}_{-1,1}-\Phi^{(1)}_{0,0}\right), \tag{31}$$

where the prefactor ensures that the conformal two-point function of the perturbing field is canonically normalized:

$$\langle\Phi(z,\bar{z})\Phi(w,\bar{w})\rangle = \frac{1}{|z-w|^{4h}}, \qquad h=\frac{2}{k+2}. \tag{32}$$

In fact, the field Φ as defined in Eqn. (31) differs from the trace adjoint defined previously by a sign, which is consistent with the form of the Hamiltonian in Eqn. (15). This sign can be identified from matching the TCSA result against the semiclassical predictions, performed in the sequel.

Using complex coordinates $\zeta=\tau+ix$, after the exponential mapping from the plane to the cylinder,

$$z = e^{2\pi\zeta/R}, \tag{33}$$

the Hamiltonian can be written as

$$H = \frac{2\pi}{R}\left(L_0+\bar{L_0}-\frac{k}{4(k+2)}\right)+\lambda\frac{2\pi}{R}\frac{R^{2-2h}}{(2\pi)^{1-2h}}\Phi(1,1). \tag{34}$$

The dimensionful coupling constant λ can be used to define a mass scale M

$$|\lambda| = M^{2-2h}. \tag{35}$$

In all our subsequent computations we use dimensionless quantities measured in units of M. The dimensionless volume parameter is given by $r = MR$ and the Hamiltonian can be written as

$$\frac{H}{M} = \frac{2\pi}{r}\left[L_0 + \bar{L_0} - \frac{k}{4(k+2)} + \text{sign}(\lambda)\frac{r^{2-2h}}{(2\pi)^{1-2h}}\Phi(1,1)\right]. \tag{36}$$

The matrix elements of the perturbing operator between descendant states can be computed by a recursive procedure using the relations given by the Kac–Moody algebra. Truncating the Hilbert space at some descendant level N, the dimensionless Hamiltonian becomes a finite numerical matrix for any given value of r, which can be diagonalized numerically, resulting in a raw TCSA spectrum that depends on the truncation level. In many cases the raw TCSA data already gives an accurate spectrum; however, we used both numerical and analytic schemes to eliminate cut-off dependence and obtain better results.

Since the perturbation is a singlet, it conserves the z component of the diagonal $SU(2)$ ($g_L = g_R$) which is

$$\mathcal{Q} = J_0^z + \bar{J}_0^z. \tag{37}$$

All eigenvalues of the charge $\mathcal{Q}$ are integers and the Hilbert space can be decomposed into sectors labeled by the eigenvalues of $\mathcal{Q}$. In all our computations we only show results for states with $\mathcal{Q} = 0$. Since the Hilbert space decomposes into integer spin representations of the diagonal $SU(2)$, each such multiplet has a single level lying in the $\mathcal{Q} = 0$ subspace. It is guaranteed analytically, but we also checked numerically that any $\mathcal{Q} \neq 0$ state is degenerate with one of the levels in the $\mathcal{Q} = 0$ subspace, and that degenerate states form full multiplets. In addition, all TCSA data we present correspond to zero-momentum states (i.e. $L_0 - \bar{L}_0 = 0$), as non-zero momentum subspaces contain no new physics.

It is also important to observe that according to the Kac–Moody fusion rules under the perturbation (Eqn. (31)), the Hilbert space (Eqn. (23)) decomposes into even and odd sectors which originate from states with j integer and half-integer, respectively. This will be important in the sequel.

3.2. Testing the TCSA

In this subsection we describe a number of tests that we put our TCSA code through. Such tests are very important as there are no exact results to verify the TCSA due to the non-integrability of the theory. The first test that we considered is specific to $k = 4$. As we have discussed, we have two realizations of $SU(2)_4 + \text{Tr}\,\Phi_{adj}$: one treating the conformal basis of $SU(2)_4$ in the language of current algebras (the picture we are focusing on in this paper) and one treating this same basis as a two boson theory, one boson with compactification radius of $\sqrt{2}\pi$ and one orbifolded boson with compactification radius of $2\sqrt{6}\pi$ (see Eqn. (5)). While these are very different starting points for the TCSA, they must lead to the same answer. And we have checked, at least in the sector of the theory containing the ground state, that they do. While this is an important check of the code, it only applies to $k = 4$. We have thus also considered the case $SU(2)_1$ perturbed with the singlet component of the $j = 1/2$ primary field (equivalent to sine-Gordon theory in the $SU(2)$ symmetric point of the attractive regime) as well as the

$k = 2$ case, where the spectrum must agree with that of three Majorana fermions; some details on this latter case are given in Subsection 4.4. Both of these tests indicate the code is working. Finally, as discussed in Subsection 3.3.4, we show that corrections to the ground state due to changing the cutoff in the theory as determined by the TCSA match those computed *analytically* using conformal field theory. This analytical computation is non-trivial and so provides another important check on whether the code is behaving as it should.

3.3. Renormalization methods

The first improvement to the raw TCSA is given by the numerical renormalization group (NRG) method introduced in [6]. The procedure consists of starting at a cut-off value where the whole matrix can be diagonalized and then incorporating higher energy levels in chunks of a given step size (number of states added at each step) until the target value of the cut-off is reached. This is necessary as the number of states grows very fast with the cut-off. For example, in the integer j sector of the $k = 4$ theory for descendant levels $N = 3, 4, 5, 6, 7$ we have 1427, 6373, 23 498, 83 144 and 264 129 zero-momentum states respectively in the $\mathcal{Q} = 0$ sector. Our computational capacity allowed us to reach the descendant level $N = 5$ with exact diagonalization, while to reach $N = 6, 7$ we have used the NRG procedure.

The next improvement takes into account the contribution of states above the cut-off using perturbation theory to second order in λ. There are several schemes in the literature that can be used, but a compromise must be struck between computational costs and accuracy. Below we give a short description of each procedure, and compare them in order to make an optimal choice for our problem.

3.3.1. Vacuum counter term

The contribution from the omitted high-energy states dependence of the ground state energy was computed using the results in [14], and the counter term necessary to eliminate the cut-off dependence to second order is given by

$$\begin{aligned}\delta E_0 &= \frac{\pi R^{3-4h}}{2(2\pi)^{2-4h}} \frac{1}{h+N+1} \left(\frac{\Gamma(2h+N+1)}{\Gamma(2h)\Gamma(N+2)} \right)^2 \\ &\quad \times {}_4F_3(1, 1+h+N, 1+2h+N, 1+2h+N; 2+N, 2+N, 2+h+N; 1) \\ &= \frac{(2\pi)^{4h-1} R^{3-4h}}{4(2h-1)\Gamma(2h)^2} N^{4h-2} + \dots \end{aligned} \tag{38}$$

with ${}_4F_3$ denoting a generalized hypergeometric function.

3.3.2. Counter terms for excited states

To eliminate cut-off dependence for excited states we can use a scheme developed in [15]. The idea is to separate the Hilbert space into a low-energy part (labeled by l), which is included in TCSA, and a high-energy part (labeled by h) which consists of states above the cut-off. For any state we split its eigenvector c into low- and high-energy parts c_l and c_h; similarly, the Hamiltonian can be split into a block form according to

$$H = \begin{pmatrix} H_{ll} & H_{lh} \\ H_{hl} & H_{hh} \end{pmatrix}. \tag{39}$$

The full eigenvalue problem can be split accordingly

$$H_{ll}c_l + H_{lh}c_h = \varepsilon c_l, \quad H_{hl}c_l + H_{hh}c_h = \varepsilon c_h, \tag{40}$$

where ε is the exact eigenvalue. Eliminating the high-energy components, c_h, gives

$$[H_{ll} \underbrace{- H_{lh}\,(H_{hh} - \varepsilon)^{-1}\,H_{hl}}_{\Delta H_{\text{full}}}]c_l = \varepsilon c_l. \tag{41}$$

We write

$$H = H_0 + V, \tag{42}$$

where H_0 is the conformal Hamiltonian and V is the matrix of the perturbing field. Note that the off-diagonal components only involve the perturbing matrix, so we obtain

$$\begin{aligned}\Delta H_{\text{full}} &= -V_{lh}(H_0 + V_{hh} - \varepsilon)^{-1}V_{hl} \\ &\approx \underbrace{-V_{lh}(H_0 - \varepsilon)^{-1}V_{hl}}_{\Delta H} + O(E_{max}^{-2}),\end{aligned} \tag{43}$$

where E_{max} is the cut-off in energy units, and we used the fact that V_{hh} only contributes at higher order. First order perturbation theory in E_{max}^{-1} gives

$$\varepsilon = E_{TCSA} + c_{TCSA}\Delta H c_{TCSA}, \tag{44}$$

where

$$H_{ll}c_{TCSA} = E_{TCSA}c_{TCSA}. \tag{45}$$

To calculate ΔH we can approximate $\varepsilon \to E_{TCSA}$ in Eqn. (43)

$$\Delta H_{ab} = -\int_{E_{max}}^{\infty} \frac{M(E)_{ab}}{E - E_{TCSA}}, \tag{46}$$

where $M(E)_{ab}$ is defined by

$$\langle a|V(\tau)V(0)|b\rangle = \int_0^{\infty} dE e^{-(E-E_a)\tau} M(E)_{ab}. \tag{47}$$

Here $V(\tau)$ is understood as a Euclidean time-evolved version of the perturbing operator,

$$V(0) = \int_0^R dx \Phi(ix). \tag{48}$$

Then one can write

$$V(\tau)V(0) = \int_0^R dx_1 \int_0^R dx_2 \Phi(ix_1 + \tau)\Phi(ix_2), \tag{49}$$

where Φ has scaling dimensions, (h, h). The leading contributions can be computed by considering the most singular terms in the operator product expansion on the cylinder

$$\Phi(ix_1 + \tau)\Phi(ix_2) \approx \sum_{\varphi} C_{\varphi\Phi\Phi}\,|ix_1 - ix_2 + \tau|^{-4h+2h_\varphi}\,\varphi(ix_2) + \ldots \tag{50}$$

where φ has scaling dimensions (h_φ, h_φ) and we only consider the first few operators. Indeed, the leading contribution is the identity with $h_1 = 0$ and $C_{1\Phi\Phi} = 1$; since we neglect the subleading terms of the identity contribution, we cannot include any operators with $h_\varphi \geq 1/2$.

In the spin 0 sector, using translation invariance of the states $|a\rangle$ and $|b\rangle$ gives

$$\begin{aligned}\langle a|\varphi(ix_2)|b\rangle &= \langle a|\varphi(0)|b\rangle \\ &= \left(\frac{2\pi}{R}\right)^{2h_\varphi} \langle a|\varphi_{plane}(1)|b\rangle. \end{aligned} \tag{51}$$

The integrals can be explicitly computed

$$\begin{aligned}\int_0^R dx_1 \int_0^R dx_2\, |ix_1 - ix_2 + \tau|^\alpha &= 2R^2\tau^\alpha {}_2F_1\left(\frac{1}{2}, -\frac{\alpha}{2}; \frac{3}{2}; -\frac{R^2}{\tau^2}\right) \\ &\quad + \frac{\tau^{2\alpha+2}}{\alpha+1} - \frac{\left(R^2+\tau^2\right)^{\alpha+1}}{\alpha+1} \\ &= \sqrt{\pi} R \frac{\Gamma\left(-\frac{\alpha+1}{2}\right)}{\Gamma\left(-\frac{\alpha}{2}\right)} \tau^{1+\alpha} + \text{less singular}. \end{aligned} \tag{52}$$

To leading order we can neglect the term $e^{E_a\tau}$ in the correlator, since the energies E we consider are above the cut-off E_{max}, while E_a is below it; similarly we can take $E_{TCSA} \to 0$ in Eqn. (46). This gives

$$\Delta H^\varphi_{ab} = \frac{(2\pi)^{4h-1} R^{3-4h} N^{4h-2h_\varphi-2}}{4(2h-2h_\varphi-1)\Gamma(2h-2h_\varphi)^2} C_{\varphi\Phi\Phi} \langle a|\varphi_{plane}(1)|b\rangle, \tag{53}$$

for the contribution coming from the operator φ in the OPE. Note that this equation gives the counter term in an operator form, in an arbitrary basis of states $|a\rangle$. The eventual correction to any given energy level is computed by evaluating its matrix in the TCSA basis and computing its expectation value with the TCSA eigenvectors corresponding to the given level at cutoff N. Note that when applied to the case of the identity, this result reproduces the leading behavior of the vacuum counter term (Eqn. (38)).

3.3.3. Running coupling

To the leading order, the counter terms (Eqn. (53)) are independent of the state under consideration and can be considered as local operators added to the Hamiltonian. This forms the basis of a renormalization group (RG) by defining a level dependent running coupling such that the counter term describing the cut-off dependence is compensated by changing the coupling. Let us denote

$$\mu = \left(\frac{2\pi}{r}\right)^{2h-2}, \tag{54}$$

and consider the case when $\varphi = \Phi$, i.e. $h_\varphi = h$. Then we can introduce a cut-off dependent coupling by requiring that the contribution of high-energy states from level N is compensated by the change in the coupling. The contribution from the Nth level to the Φ term in the Hamiltonian is just the derivative of Eqn. (53) with respect to N (to leading order in $1/N$), which is equal to

$$\Delta H^{\Phi}_{ab} = \frac{2\pi}{r}\mu^2 \frac{\pi C_{\Phi\Phi\Phi}}{\Gamma(h)^2} N^{2h-3} \langle a|\Phi_{plane}(1)|b\rangle. \tag{55}$$

We make the coupling depend on N and stipulate that it is evolved from N to $N-1$ by including the counter term's contribution. This leads to the RG equation of the form used in [7,12,13]

$$\mu_N = \mu_{N-1} + \mu^2_{N-1} \frac{\pi C_{\Phi\Phi\Phi}}{\Gamma(h)^2} N^{2h-3} + \dots \tag{56}$$

where the dots denote terms subleading for large N, which can be integrated to

$$\mu_\infty = \frac{\mu_N}{1 + C_1 \mu_N N^{2h-2}}, \qquad C_1 = \frac{2\pi C_{\Phi\Phi\Phi}}{(4h-4)\Gamma(h)^2}, \tag{57}$$

to leading order for large N. Let us denote the dimensionless energy levels by $e_i(r)$, which are just the eigenvalues of the dimensionless TCSA Hamiltonian (Eqn. (36)) as functions of r, with the vacuum being $e_0(r)$.

This RG equation, inasmuch as it can be derived from the invariance of the partition function under changes in coupling [12], expresses the RG invariance of the gaps of the form:

$$E_i(\lambda_\infty) = E^{(N)}_i(\lambda_N). \tag{58}$$

Due to Eqn. (54), this invariance can be reinterpreted in terms of the dimensionless energy levels via

$$e_i(r_\infty) = \frac{r_N}{r_\infty} e^{(N)}_i(r_N), \tag{59}$$

where e_i are the energy levels at cut-off $N = \infty$. Note that the energy also needs to be rescaled due to the $1/r$ prefactor in the dimensionless TCSA Hamiltonian (Eqn. (36)).

We remark that at higher orders in $1/N$ the counter terms (and therefore the running coupling as well) are state dependent [13]. One way to take this into account is to compute the full counter term (Eqn. (44)) without using the approximation of the previous subsection, i.e. keeping the dependence on E_{TCSA} and E_a in Eqns. (46) and (47). This leads to a rather complicated and computationally expensive method even for the counter terms themselves, and it makes rather difficult the implementation and solution of the corresponding renormalization group equations, which describe non-local Hamiltonian terms [15]. Henceforth we neglect these higher corrections in our computations.

3.3.4. Renormalizing the ground state

The ground state of the theory has the conformal vacuum as its ultraviolet limit, and is contained in the even, $\mathcal{Q} = 0$, zero-momentum sector. In Fig. 2 we show results coming from NRG + TCSA, the effect of the vacuum counter term (Eqn. (38)), as well as the results obtained by implementing both the counter term and the running coupling according to Eqn. (59). In small volume we can see that the counter terms at different cut-off levels scale the energy level to the same curve, verifying that the subtraction provides reliable results even when starting from NRG + TCSA data with low values of the cut-off. Note that taking into account the running coupling gives a further significant reduction of cut-off dependence. This scaling is one of the verification tools we used to affirm our belief that our code is producing correct results.

The slope extracted from the linear regime of the vacuum level gives the ground state (bulk) energy density $\mathcal{E}_0$, and can be estimated by fitting a linear function in the appropriate range of volume. The resulting estimates are given in Table 1.

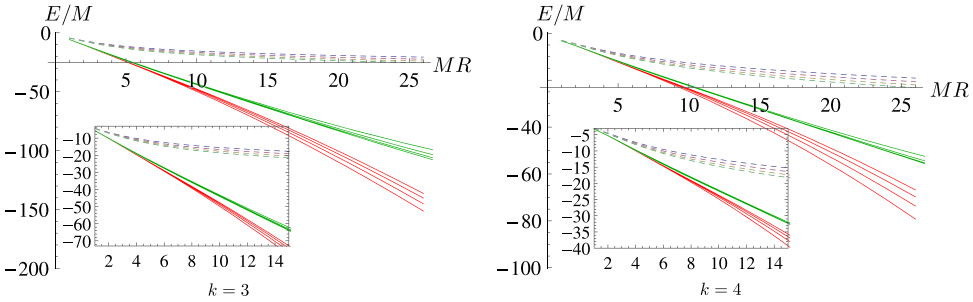

Fig. 2. $k = 3$ (left) and 4 (right), $\lambda > 0$ ground state energy data obtained by TCSA + NRG for cutoff levels $N = 5, 6, 7, 8$ and $N = 4, 5, 6, 7$ (dashed lines); the results with the counter term (Eqn. (38)) (red lines); and the data involving the counter term and the RG improvement (Eqn. (59)) (green lines). The insets show the same results blown up on the $1 < L < 14$ interval. Note that in the direction of increasing cut-off N the subtracted (red), and the subtracted and renormalized (green) levels move less as the cut-off grows, which is a further confirmation of the validity of the renormalized TCSA. (For interpretation of the references to color in this figure, the reader is referred to the web version of this article.)

Table 1
The bulk energy density $\mathcal{E}_0$ given in units of M (cf. Eqn. (35)).

$\mathcal{E}_0$	$\lambda > 0$	$\lambda < 0$
$k = 3$	-4.55 ± 0.01	-7.69 ± 0.01
$k = 4$	-2.21 ± 0.01	-5.03 ± 0.01

3.3.5. Numerical application of the renormalization methods

To eliminate the additive bulk energy renormalization (Eqn. (38)) we consider the gaps relative to the vacuum. The running coupling (Eqn. (57)) leads to the renormalization prescription

$$e_i(r_\infty) - e_0(r_\infty) = \frac{r_N}{r_\infty}\left(e_i^{(N)}(r_N) - e_0^{(N)}(r_N)\right), \tag{60}$$

which we call the RC (running coupling) correction. It is also possible instead to add the counter terms (Eqn. (53)) where we can include the contribution of all operators φ below a certain h_φ chosen to keep the slowest-decaying contributions (in practice we chose to incorporate the primary contributions). This will be called the CT (counter term) correction. The difference between the two corrections is that in contrast to the CT correction, the RC correction only involves a single operator contribution, however by introducing the running coupling it sums up the leading power in the cut-off dependence to any order.

We illustrate the renormalization method for the first excited level for $k = 4$ and $\lambda > 0$, which comes from the odd sector and consists of three degenerate states with $\mathcal{Q} = +1, 0, -1$ forming a triplet under diagonal $SU(2)$. We consider the state corresponding to a stationary particle, which can be found in the zero-momentum sector. For higher cut-offs we find that the two prescriptions converge to each other as illustrated in Fig. 3, so we can use the computationally simpler RC method to obtain renormalized results.

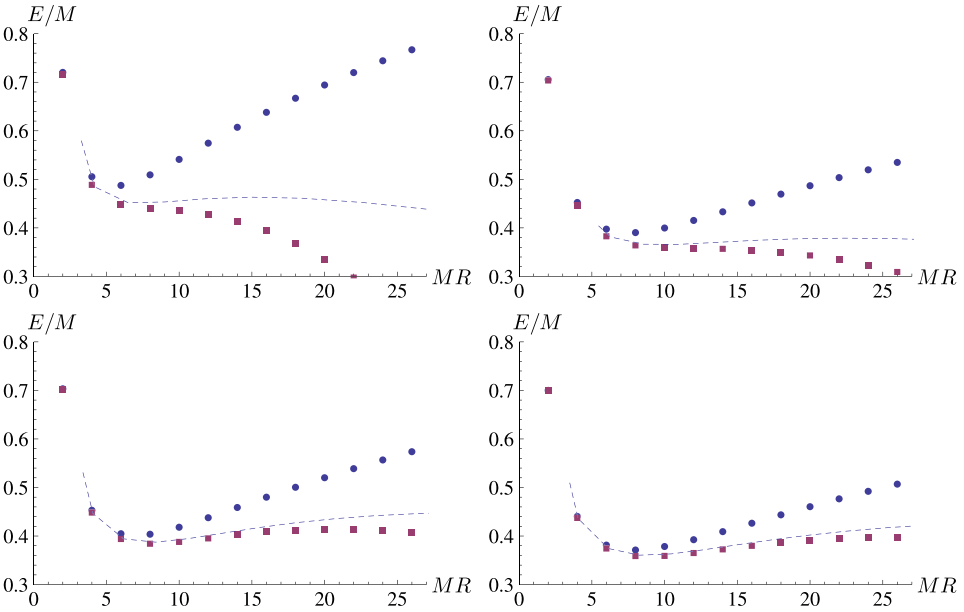

Fig. 3. Finite volume gap in the perturbed $SU(2)_4$ model for $\lambda > 0$ at cut-offs $N = 2$, 3, 4 and 5. The plot shows the raw TCSA data (without NRG, blue circles), and those after the RC (dashed lines) and the CT (magenta squares) corrections were applied. The gap can be estimated to be $\Delta = 0.36 \pm 0.03$, and the error is approximated by the difference between the gap estimates for $N = 3$ and 6. (For interpretation of the references to color in this figure, the reader is referred to the web version of this article.)

4. Numerical results for the spectrum

4.1. The $\lambda < 0$ case

In this regime we expect two triplets of weakly interacting particles that have a mass given by Eqn. (11). We show the spectra of zero-momentum $\mathcal{Q} = 0$ states relative to the absolute ground state in Fig. 4 which clearly show a doubly degenerate vacuum structure. In finite volume, the degeneracy of the vacua is lifted by the tunneling, which vanishes exponentially with the volume. Due to the $\mathbb{Z}_2$ symmetry relating the two vacua $|1\rangle$ and $|2\rangle$, the finite volume ground states are given by

$$|\pm\rangle = \frac{1}{\sqrt{2}}\left(|1\rangle \pm |2\rangle\right), \tag{61}$$

and are expected to emerge from the even and odd sectors, respectively. Since we plot the energies relative to the absolute finite volume ground state $|+\rangle$, the presence of these vacua is signaled by a state originating from the odd sector with a relative energy approaching zero exponentially with the volume.

As expected from the semiclassical considerations, the first excitations are indeed a triplet of particles, and they too appear in two copies according to the vacua. Their triplet nature can be seen both by looking in the $\mathcal{Q} = \pm 1$ sectors for the other components of the multiplets, but also from the fact that the energy levels in the ultraviolet ($mR \sim 0$) limit are seen to emerge from conformal states transforming as a triplet under the diagonal $SU(2)$. In particular, the lowest

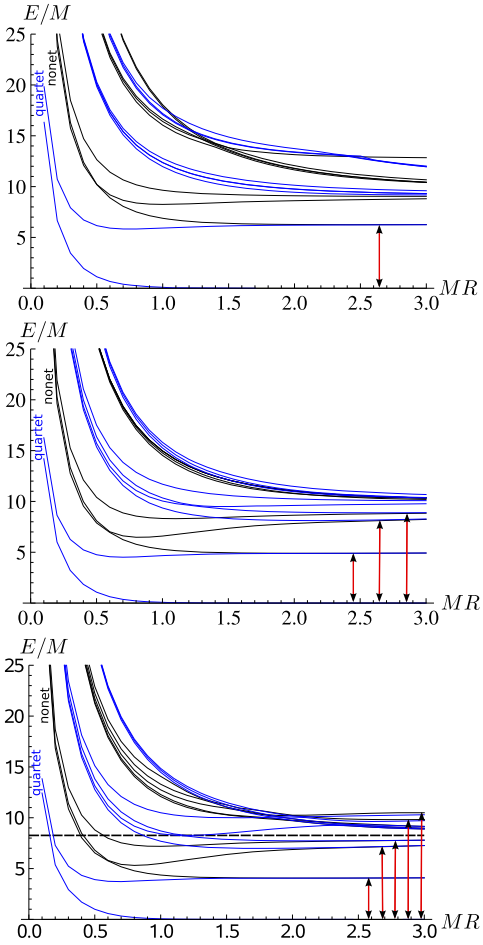

Fig. 4. Finite volume spectra in the perturbed $SU(2)_k$ models with $k = 3, 4, 5$ for negative coupling constant at cut-offs $n_{max} = 7, 6, 5$, respectively. We show raw TCSA data since renormalization here had an effect that is not visible on these figures. Colors represent energy levels in the integer (black) and half integer (blue) sectors. The red arrows show the gaps corresponding to one-particle states. For $k = 5$, two of these are already higher than the two-particle threshold (shown as the thick dashed line), and due to non-integrability they are expected to correspond to resonances. (For interpretation of the references to color in this figure, the reader is referred to the web version of this article.)

lying states come from a quartet of states created by the primary field $\Phi^{(1/2)}$ and a nonet of states created by the primary field $\Phi^{(1)}$. Under the global $SU(2)$, the quartet decomposes as

$$\frac{1}{2} \otimes \frac{1}{2} = 0 \oplus 1, \tag{62}$$

with the singlet giving the second vacuum state, while the triplet corresponds to the first triplet of one-particle states. In the plots of Fig. 4 the quartet corresponds to the first two blue lines (their color indicates that they come from a sector created by a primary field with half-integer j).

The nonet

$$1 \otimes 1 = 0 \oplus 1 \oplus 2, \tag{63}$$

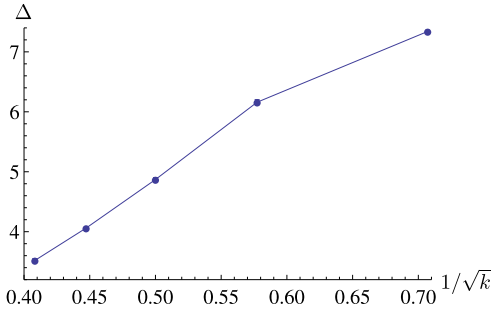

Fig. 5. TCSA mass gap for negative coupling constant as a function of $k^{-1/2}$. We show data coming from $k = 2$, 3, 4 and 5 models. We also put error bars on the data points which we calculated by subtracting the gap estimates with and without applying the RC improvement, but they are so small that they are practically invisible in the plot.

contains the other triplet of one-particle levels while the single and quintet are excited states. They correspond to the lowest three black levels visible in the plots, which are exactly (the $\mathcal{Q} = 0$ components of) the three multiplets. Of these three levels, the one corresponding to the triplet 1 in Eqn. (63) approaches the other (blue) triplet from Eqn. (62) exponentially with increasing volume. They also level out exponentially, signaling that these are single-particle states, coming in two copies according to the degenerate vacua.

In Fig. 5 we show that for larger values of k the gap measured from the flat portion of the first one-particle levels indeed follows the $k^{-1/2}$ scaling of the particle mass expected from the semiclassical arguments. The spectra also show the presence of additional states below the two-particle threshold. Due to the double degenerate vacua, one expects kinks interpolating between them. With the periodic boundary conditions imposed by TCSA one can only see states with an even number of kinks such that the sequence of vacua interpolated by them has the same starting and end points. In addition, these kinks are also expected to have bound states, and the lowest lying particle triplet can be identified with the lowest mass kink–antikink bound states.

In the absence of more detailed knowledge about the theory, at present we cannot identify the higher states conclusively, but it seems that at least the first few levels very much resemble the breather doublets seen in the 2-folded sine-Gordon theory [35], so it is likely that these are indeed higher kink–antikink bound states beyond the lowest triplet. These levels can be seen in Fig. 4 as pairs of black and blue lines approaching each other and also leveling out exponentially at the same time. The fact that one of these always comes from the even, while the other from the odd sector (as shown by their colors) confirms the interpretation that these are indeed two copies of higher kink–antikink bound state multiplets (note that these are not necessary triplets; from the identification of the nonet lines we know the next two are a singlet and a quintuplet).

One can also see that the number of such one-particle level candidates increases with k, which is what is expected in the semiclassical limit [36,37]. In addition, the characteristic dependence of the lowest particle mass on k suggests that the mass scale M is related to the kink mass, and that the spectrum of bound states becomes dense for large k, analogously to the Φ^4 and sine-Gordon models treated in [36,37]. Due to non-integrability of the model it is also expected that two-kink bound states over the two-particle threshold are in fact resonances whose finite volume signatures must resemble those in the two-frequency sine-Gordon theory studied in [38]; however, our data do not allow a reliable identification of these signatures at present. We also remark that in spite of non-integrability, there are also apparent level crossings in the spectra, e.g. between even (black) and odd (blue) levels since they do not mix under the perturbation. The additional higher states

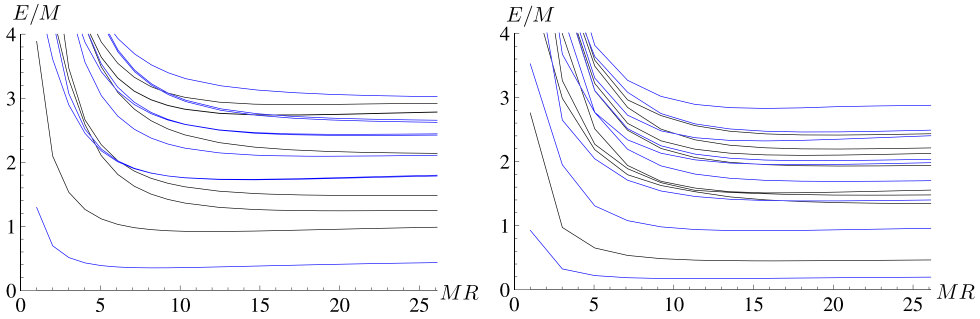

Fig. 6. Spectra in the $k = 4$ and 6 models for $\lambda > 0$ at cut-offs $N = 7$ and 4. Data was improved by the RC method. Colors represent level data obtained in the integer (black) and half integer (blue) sectors. (For interpretation of the references to color in this figure, the reader is referred to the web version of this article.)

can be interpreted as two- and more particle levels composed of particles and/or even number of kinks.

4.2. $\lambda > 0$, *even* k

In Fig. 6 we show the results for positive λ and even level k. We observe a single vacuum and a triplet of one-particle levels, which are consistent with the effective σ-model picture based on the action in Eqn. (13). From the first excited levels alone, the gaps can be estimated as $\Delta = 0.37 \pm 0.03$ and $\Delta = 0.18 \pm 0.02$ for $k = 4$ and 6, respectively, which are much smaller than those for $\lambda < 0$ and decrease strongly with increasing k as expected from the semiclassical result (Eqn. (14)). Unfortunately, the numerical accuracy for higher levels is not very good, which at this stage precludes their interpretation; this is further complicated by the smallness of the gaps, which means that the volumes we could reach are in fact very small in terms of the correlation length, therefore sizable exponential finite size effects are expected.

For $k = 4$, the two-particle gap can be seen to be of order 0.9 from the lowest level above the one-particle state; this is roughly consistent with the gap estimate above, but cannot be trusted to be of the same precision as there are clear signals of large residual cut-off dependence in the behavior of the level, e.g. the fact that it curves upwards for larger values of mR, while in reality a two-particle level must approach the threshold from above with a behavior $(mR)^{-2}$. For the case $k = 6$, the truncation achieved is very low and so the higher levels cannot be trusted, precluding their analysis for the time being.

4.3. $\lambda > 0$, *odd* k

In this regime, as we discussed in Section 2, we expect a massless flow to an $SU(2)_1$ low-energy fixed point. The mass scale (Eqn. (14)) in this case corresponds to the cross-over scale. The spectra shown in Fig. 7 do show marked differences from the even k case. All levels are monotonically decreasing with the volume, rather than leveling out as in a massive spectrum. Also, one would expect the gap for $k = 3$, 5 larger than for $k = 4$, 6, respectively, while compared to the data in Fig. 6 one readily sees that the distance between the ground state and the first excited state is, instead, markedly smaller and monotonically decreasing even at the largest volume shown.

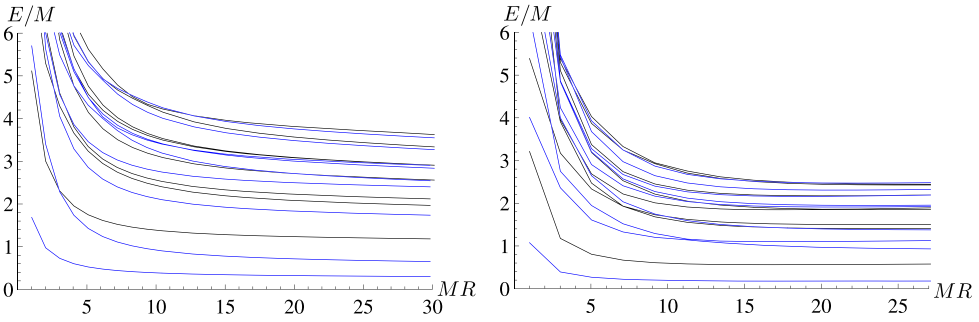

Fig. 7. Spectra for $k = 3, 5$ for positive coupling constant at cut-offs $N = 8$ and 6. Data was improved by the RC method. Colors represent level data obtained in the integer (black) and half integer (blue) sectors. (For interpretation of the references to color in this figure, the reader is referred to the web version of this article.)

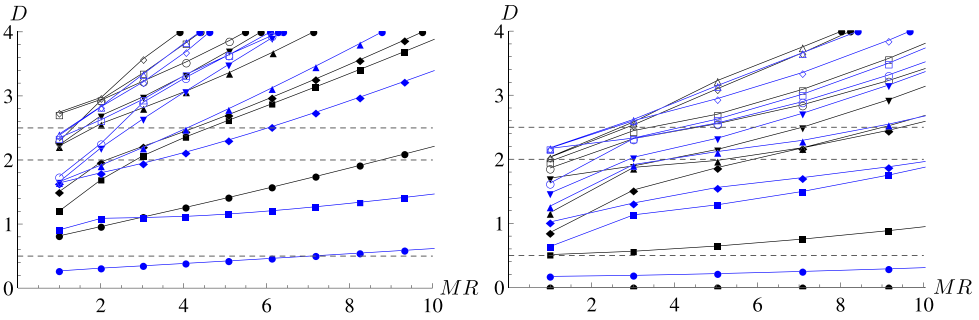

Fig. 8. Same data as in Fig. 7, but here we show the scaling functions, $D_i = \frac{R}{2\pi}(E_i - E_0)$. The dashed lines are the first few scaling weights in the $SU(2)_1$ CFT.

The existence of an infrared fixed point implies that for large values of the volume the energy levels should behave as

$$E_i - E_0 \sim \frac{2\pi x_i}{R} + \dots$$

where x_i are scaling dimensions in the $SU(2)_1$ theory, and the dots indicate corrections to the low-energy scaling limit. One can define the scaling functions

$$D_i = \frac{R}{2\pi}(E_i - E_0) = x_i + \dots$$

As shown in Fig. 8, the detailed matching is rather limited. There are reasons for which this is expected. First, from the gaps measured for even k, the typical scale parameter for the cross-over is expected to be $MR \gtrsim 4$. In addition, the cross-over itself is slow, due to the fact that the irrelevant perturbation describing the incoming direction in the infrared is the current–current perturbation of $SU(2)_1$, which is only marginally irrelevant and leads to a logarithmic approach to the fixed point [40]. Therefore one expects that the fixed point would only be observable for volume values much higher than allowed by TCSA accuracy.

It has long been known that observing an infrared fixed point in TCSA is difficult [39]. In Ref. [39] an attempt was made to observe the flow from the tricritical Ising conformal minimal model to the Ising minimal model by perturbing the tricritical Ising theory with the subleading

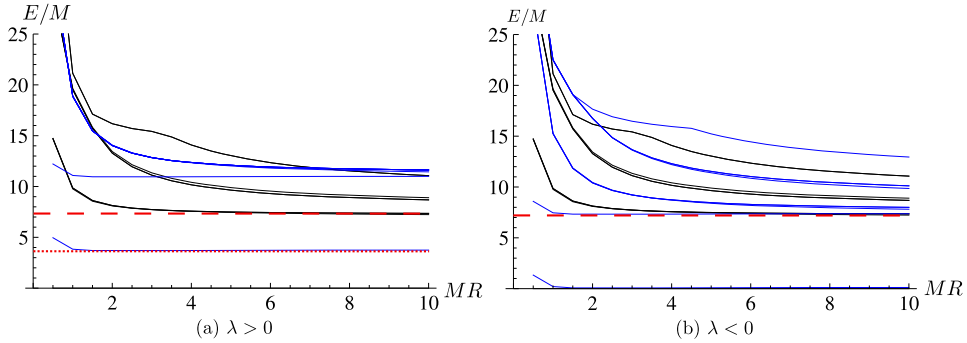

Fig. 9. Spectra for $k = 2$. The red dotted line (shown only for $\lambda > 0$) corresponds to the fermion mass $m = 2\pi M/\sqrt{3}$, while the red dashed lines show the position of the two-particle threshold $2m$. (For interpretation of the references to color in this figure, the reader is referred to the web version of this article.)

energy perturbation, with the conclusion that the behavior of the first excited state was not inconsistent with the existence of the fixed point. In a study of two-frequency sine-Gordon model [4], the Ising fixed point was just barely in the reach of the TCSA. In that case however, the sine-Gordon frequency provided a parameter which could be tweaked to improve convergence to the point that the first two scaling dimensions of the infrared fixed point could be extracted, albeit with considerable errors. Note also that in these examples the approach to the fixed point was much faster (given by power corrections).

Pending more accurate TCSA numerics (which would require a more accurate modeling of the cut-off dependence, and more computing power to allow higher truncation levels), we can only say that the TCSA data are qualitatively consistent with the existence of a low-energy quantum critical point, and the first scaling function in Fig. 8 is also roughly consistent with the lowest scaling weight

$$x_1 = \frac{1}{2}.$$

4.4. The case $k = 2$

For this case one expects a spectrum of free massive Majorana fermions; in our units given by Eqn. (35) the fermions mass is

$$m = \frac{2\pi}{\sqrt{3}} M. \tag{64}$$

The resulting spectra for $\lambda > 0$ and $\lambda < 0$ are shown in Fig. 9. They are exactly the spectra expected for three Majorana fermions in the $\mathbb{Z}_2$ symmetric and $\mathbb{Z}_2$ symmetry breaking phases, respectively. Note that in the $\lambda < 0$ the excitations are kinks, therefore there are no single-particle levels and every multi-kink level appears in two copies (one even, the other odd), which are split by tunneling effects decaying exponentially with volume. There are no kink–antikink bound states below the two-particle threshold. For the $\lambda < 0$, the $k = 2$ point is analogous to the free-fermion point of sine-Gordon theory, while the $k > 2$ cases correspond to attractive regime. The main difference from the sine-Gordon case is the non-integrability and the presence of $SU(2)$ invariance.

In the symmetric phase $\lambda > 0$, there is a unique vacuum and the even/odd sectors correspond to levels with even/odd fermion numbers. In particular, the odd sector does contain one-particle states.

5. Summary and conclusions

We have studied the $SU(2)_k + \mathrm{Tr}\,\Phi_{adj}$ theory using the TCSA + RG approach. We have compared our numerical results to the semiclassical analysis of this model. We recall that the semiclassical picture suggests two regimes. One of them corresponds to the negative sign of the coupling and has a doubly degenerate ground state characterized by a nonzero vacuum average of the $SU(2)$ matrix field $\langle \mathrm{Tr}\, g\rangle = \pm\sigma$. Therefore one expects kinks interpolating between the different vacua. Indeed TCSA data show a spectrum that resembles those in the Φ^4 and also the 2-folded sine-Gordon theory, where particles arise as bound states of kinks with a spectrum that becomes dense in the semiclassical limit which corresponds here to large k. The lowest lying excited states consist of two triplets of particles with the same mass and can be identified with the lightest kink–antikink bound states.

In the other regime for even k the semiclassical considerations suggest a triplet of massive excitations, whose low-energy dynamics is governed by the $O(3)$ sigma model. The presence of a single vacuum with a massive triplet is confirmed by TCSA, but the precision is significantly smaller since due to the much smaller gap, it is necessary to go to much larger volumes which increases the truncation effects. Even so, the vacuum energy density and the mass gap can still be extracted with a reasonable accuracy by applying renormalization group improvement techniques. For odd k, the semiclassical considerations imply the presence of a low-energy quantum critical point described by the $SU(2)_1$ conformal field theory. The TCSA data are consistent with this prediction, but are not accurate enough to identify the nature of the fixed point conclusively. We still think that the semiclassical picture has proven robust enough so that this prediction can be trusted.

For the exactly solvable case $k = 2$ the spectrum of the model describes three Majorana fermions which also constitute a triplet. The model is then non-interacting, therefore there are no more particles in the spectrum. For the two signs of the coupling the spectrum differs as usual for a free fermion theory, and fits well into the pattern observed for $k > 2$.

Acknowledgements

R.M.K. and A.M.T. are supported by the US DOE under contract number DE-AC02-98 CH 10886. R.M.K. also received support from by the National Science Foundation under grant No. PHY 1208521. G.T. and T.P. are supported by Hungarian Academy of Sciences both by Momentum grant LP2012-50/2013 and a postdoctoral fellowship for T.P.

Appendix A. Realization of $SU(2)_k + \mathrm{Tr}\,\Phi_{adj}$

Here we give an example of how the perturbed WZNW model of Eqn. (1) can appear in the context of an electronic model. We start with a lattice model with $U(1) \times SU(2) \times SU(k)$ symmetry [23],

$$H = \sum_n \Big\{ -t\Big[\psi^\dagger_{j\sigma}(n+1)\psi_{j\sigma}(n) + H.c.\Big]$$

$$+ U \sum_{\{j\sigma\}\neq\{i\sigma'\}} [\psi^\dagger_{j\sigma}(n)\psi_{j\sigma}(n)][\psi^\dagger_{i\sigma'}(n)\psi_{i\sigma'}(n)]$$
$$- J\psi^\dagger_{j\sigma}(n)\psi_{i\sigma}(n)\psi^\dagger_{i\sigma'}(n)\psi_{j\sigma'}(n)\Big\}, \tag{A.1}$$

where $\psi^\dagger_{j\sigma}(n)$ and $\psi_{j\sigma}(n)$ are creation and annihilation operators of electrons located at sites n; $\sigma = \pm 1/2$ are spin and $i, j = 1, \ldots, k$ are orbital indices. Treating the interaction as small in comparison with the Fermi energy and assuming that the band is far from being half filled, we separate fast and slow Fourier harmonics of the electron operators:

$$\psi(n) = \mathrm{e}^{-ik_F n a_0} R(x) + \mathrm{e}^{ik_F n a_0} L(x), \quad x = n a_0, \tag{A.2}$$

where k_F is the Fermi wave vector and a_0 is the lattice constant, and arrive to the continuum version of Eqn. (A.1) in the form of the chiral Gross–Neveu model with the most general current–current interaction. The corresponding Hamiltonian density is

$$\mathcal{H} = \mathrm{i}v(-R^\dagger_{\sigma j}\partial_x R_{\sigma j} + L^\dagger_{\sigma j}\partial_x L_{\sigma j}) + g_c R^\dagger_{\sigma j} R_{\sigma j} L^\dagger_{\sigma' p} L_{\sigma' p}$$
$$+ g_o R^\dagger(\tau^a \otimes I) R L^\dagger(\tau^a \otimes I) L + g_{so} R^\dagger(\tau^a \otimes \sigma^b) R L^\dagger(\tau^a \otimes \sigma^b) L$$
$$+ g_s R^\dagger(I \otimes \sigma^a) R L^\dagger(I \otimes \sigma^a) L, \tag{A.3}$$

where σ^a $(a = 1, 2, 3)$ acting on the Greek indices and τ^a $(a = 1, \ldots, k^2 - 1)$ acting on the Latin indices are generators of the $su(2)$ and $su(k)$ algebras respectively, normalized as

$$\mathrm{Tr}(\sigma^a \sigma^b) = \mathrm{Tr}(\tau^a \tau^b) = \frac{\delta_{ab}}{2}.$$

The coupling constants $g_{1,2,3}$ are related to U and J while v the Fermi velocity is given by $v = 2t \sin(k_F a_0)$.

Model (Eqn. (A.3)) is integrable for $g_o = g_{so}/2$, $g_s = g_{so}/k$ where in the case the symmetry expands to $U(1) \times SU(2k)$. In this case the abelian sector is massless and the non-abelian sector is massive if at least one of g_o or g_s is positive and $g_{so} \neq 0$ and is massless otherwise. It is also integrable if $g_{so} = 0$. For this last case the Hamiltonian density can be written as a sum of three independent Wess–Zumino–Novikov–Witten (WZNW) models perturbed by the current–current interactions:

$$\mathcal{H} = \Big[\frac{2\pi}{k+2}\Big(:J^a_R J^a_R: + :J^a_L J^a_L:\Big) + g_s J^a_R J^a_L\Big] \tag{A.4}$$
$$+ \Big[\frac{2\pi}{k+2}\Big(:F^a_R F^a_R: + :F^a_L F^a_L:\Big) + g_o F^a_R F^a_L\Big] \tag{A.5}$$
$$+ \Big[\frac{\pi}{k}\Big(:j_R j_R: + :j_L j_L:\Big) + g_c j_R j_L\Big], \tag{A.6}$$

where $J^a_{R/L}$, $F^a_{R/L}$, and $j_{R/L}$ are $SU(2)_k$, $SU(k)_2$ and $U(1)$ left/right Kac–Moody currents. Each perturbed WZNW model is exactly solvable [21,25].

We consider the case $g_s < 0$ and small g_{so} when the term mixing the spin and the orbital sectors in Eqn. (A.3) can be considered as a perturbation around the $SU(2)_k$ WZNW critical point. As we shall demonstrate, this perturbation is always relevant and is given by the $SU(2)_k$ adjoint operator.

The standard analytic approach to the models of type (Eqn. (A.3)) starts with RG equations. On this basis certain robust predictions have been made [26,27]. In particular it has been argued that at the lowest energies the largest possible symmetry is restored (in our case it would be

$U(1) \times SU(2k)$). We do note that the reliability of such approach hinges in part on weak coupling as the Gell-Mann–Low function is universal only at first loop. The first loop RG equations for the model in Eqn. (A.3) are [24]

$$\dot{g}_o = k g_o^2 + 3k g_{so}^2/4,$$
$$\dot{g}_{so} = (k-2) g_{so}^2 + g_{so}(k g_s + 2 g_o), \quad \dot{g}_s = 2 g_s^2 + 2(k - 1/k) g_{so}^2. \tag{A.7}$$

The case we are interested in is $g_o(0) > 0, g_s(0) < 0$. Then at $g_{so} = 0$ the current–current interaction in the $SU(2)$ invariant sector scales to zero and this sector is gapless. On the other hand, the interaction in the $SU(k)$ sector (the orbital one) scales to strong coupling and the excitations in this sector become massive. This occurs at the RG scale $\xi_o \approx 1/g_o(0)k$. At finite g_{so} the corresponding term acts as a relevant perturbation. Assuming that g_{so} remains the smallest in flowing to the scale governed by ξ_o, we extract from Eqn. (A.7) its value at this scale to be:

$$g_{so}(\xi_o) \approx \frac{g_{so}(0)}{g_o(0) + 2|g_s(0)|/k}. \tag{A.8}$$

We will assume that $|g_{so}(\xi_o)| \ll 1$ and consider the spin–orbit current–current interaction as a perturbation. As it was demonstrated in [17], this perturbing operator is the trace of the primary field Φ^{adj}_{AB} of the $SU(2)_k$ WZNW model where Φ^{adj}_{AB} is the field belonging to the adjoint representation. This argument is based on the observation that the marginally relevant term with g_{os} having scaling dimension 2 can be represented as a product of conformal blocks of the $SU(k)_2$ and $SU(2)_k$ primary fields in the adjoint representation. This suggestion is based on their scaling dimensions:

$$d_{adj}[SU(k)_2] = \frac{2k}{k+2}, \quad d_{adj}[SU(2)_k] = \frac{4}{k+2}. \tag{A.9}$$

In the vacuum of the perturbed $SU(k)_2$ WZNW theory, only the $\mathrm{Tr}\,\Phi^{adj}$ has a nonzero average. This leads one to the conclusion that after the high energy degrees of freedom of this theory are integrated out, the local operator $\mathrm{Tr}\,\Phi^{adj}[SU(2)_k]$ will emerge from the product of the corresponding conformal blocks.

We thus estimate the coupling of the perturbation to be equal to

$$\lambda \sim g_{so}(\xi_0) \langle \mathrm{Tr}\,\Phi^{adj}[SU(k)] \rangle. \tag{A.10}$$

As is shown in the main text, the physics of the model in Eqn. (1) depends crucially on the sign of λ. If we consider the WZNW action in Eqn. (1) as a descendant of the fermionic model (Eqn. (A.3)), the sign is determined by the product of signs of g_{so} and the vacuum average of the adjoint operator in the $SU(k)$ sector (Eqn. (A.10)). The ground state of the $SU(k)_2$ model perturbed by the current–current interaction is degenerate and hence the magnitude and the sign of λ depend on the vacuum. This degeneracy is lifted by the interaction with the $SU(2)$ sector. As a result the sign of the interaction (Eqn. (A.10)) must be chosen so as to minimize the ground state energy. As we have demonstrated (cf. Table 1), for a given k the ground state energy is always lower for $\lambda < 0$ where the masses in the $SU(2)$ sector are the largest and the lowest energy excitations consist of a massive triplet of particles, which appear in two copies due to the degenerate pair of vacua.

References

[1] P. Fonseca, A. Zamolodchikov, J. Stat. Phys. 110 (2003) 527.

[2] G. Delfino, P. Grinza, G. Mussardo, Nucl. Phys. B 737 (2006) 291.
[3] G. Delfino, G. Mussardo, Nucl. Phys. B 516 (1998) 675, arXiv:hep-th/9709028;
G. Delfino, G. Mussardo, P. Simonetti, Nucl. Phys. B 473 (1996) 469.
[4] Z. Bajnok, L. Palla, G. Takács, F. Wágner, Nucl. Phys. B 601 (2001) 503, arXiv:hep-th/0008066.
[5] V.P. Yurov, Al.B. Zamolodchikov, Int. J. Mod. Phys. A 6 (1991) 4557.
[6] R.M. Konik, Y. Adamov, Phys. Rev. Lett. 98 (2007) 147205.
[7] R.M. Konik, Phys. Rev. Lett. 106 (2011) 136805.
[8] R.M. Konik, M.Y. Sfeir, J.A. Misewich, Phys. Rev. B 91 (2015) 075417.
[9] J.-S. Caux, R.M. Konik, Phys. Rev. Lett. 109 (2012) 175301.
[10] G.P. Brandino, J.-S. Caux, R.M. Konik, arXiv:1407.7167.
[11] A. Coser, M. Beria, G. Brandino, R.M. Konik, G. Mussardo, J. Stat. Mech. (2014) P12010.
[12] G. Feverati, K. Graham, P.A. Pearce, G.Zs. Toth, G. Watts, arXiv:hep-th/0612203.
[13] P. Giokas, G. Watts, arXiv:1106.2448 [hep-th].
[14] M. Lencsés, G. Takács, J. High Energy Phys. 1409 (2014) 052, arXiv:1405.3157 [hep-th].
[15] M. Hogervorst, S. Rychkov, B.C. van Rees, Phys. Rev. D 91 (2015) 025005, arXiv:1409.1581 [hep-th].
[16] P. Lecheminant, A.M. Tsvelik, Phys. Rev. B 91 (2015) 174407, arXiv:1502.04515.
[17] S. Akhanjee, A.M. Tsvelik, Phys. Rev. B 87 (2013) 195137.
[18] H. Nonne, P. Lecheminant, S. Capponi, G. Roux, E. Boulat, Phys. Rev. B 84 (2011) 125123, arXiv:1107.0171 [cond-mat.quant-gas].
[19] V. Bois, S. Capponi, P. Lecheminant, M. Moliner, K. Totsuka, Phys. Rev. B 91 (2015) 075121, arXiv:1410.2974 [cond-mat.str-el].
[20] A.M. Tsvelik, Phys. Rev. B 42 (1990) 10499.
[21] A.M. Tsvelik, Sov. Phys. JETP 66 (1987) 754.
[22] V.A. Fateev, Int. J. Mod. Phys. A 6 (1991) 2109.
[23] Z.P. Yin, K. Haule, G. Kotliar, Phys. Rev. B 86 (2012) 195141.
[24] C. Aron, G. Kotliar, Phys. Rev. B 91 (2015) 041110(R).
[25] F.A. Smirnov, Int. J. Mod. Phys. A 9 (1994) 5121.
[26] L. Balents, M.P.A. Fisher, Phys. Rev. B 53 (1996) 12133;
H.H. Lin, L. Balents, M.P.A. Fisher, Phys. Rev. B 56 (1997) 6569.
[27] R.M. Konik, H. Saleur, A.W.W. Ludwig, Phys. Rev. B 66 (2002) 075105.
[28] I. Affleck, Nucl. Phys. B 305 (1988) 582.
[29] D.G. Shelton, A.A. Nersesyan, A.M. Tsvelik, Phys. Rev. B 53 (1996) 8521.
[30] A.B. Zamolodchikov, Al.B. Zamolodchikov, Ann. Phys. 120 (1979) 253.
[31] P.B. Wiegmann, Phys. Lett. B 152 (1985) 209;
P.B. Wiegmann, JETP Lett. 41 (1985) 95.
[32] V.A. Fateev, Al.B. Zamolodchikov, Phys. Lett. B 271 (1991) 91.
[33] M. Beria, G.P. Brandino, L. Lepori, R.M. Konik, G. Sierra, Nucl. Phys. B 877 (2013) 457, arXiv:1301.0084 [hep-th].
[34] A.B. Zamolodchikov, V.A. Fateev, Sov. J. Nucl. Phys. 43 (1986) 657, Yad. Fiz. 43 (1986) 1031.
[35] Z. Bajnok, L. Palla, G. Takács, F. Wágner, Nucl. Phys. B 587 (2000) 585, arXiv:hep-th/0004181.
[36] R.F. Dashen, B. Hasslacher, A. Neveu, Phys. Rev. D 11 (1975) 3424.
[37] G. Mussardo, Nucl. Phys. B 779 (2007) 101.
[38] B. Pozsgay, G. Takács, Nucl. Phys. B 748 (2006) 485, arXiv:hep-th/0604022.
[39] M. Lassig, G. Mussardo, J.L. Cardy, Nucl. Phys. B 348 (1991) 591.
[40] J.L. Cardy, J. Phys. A 19 (1986) L1093.